ISBN: 978-3-95450-204-2 ISSN: 2673-5350 doi:10.18429/JACoW-IBIC2019-MOPP038

THE BEAM DIAGNOSTICS TEST BENCH FOR THE COMMISSIONING OF THE PROTON LINAC AT FAIR

S. Udrea†, P. Forck, C. M. Kleffner, K. Knie, T. Sieber, GSI Helmholtzzentrum für Schwerionenforschung GmbH, Darmstadt, Germany

Abstract

A dedicated proton injector for FAIR (the pLinac) is presently under construction at GSI Darmstadt. This accelerator is designed to deliver a beam current of up to 70 mA with a final energy of 68 MeV for the FAIR anti-proton program. For the commissioning of the pLinac a movable beam diagnostics test bench will be used to characterize the proton beam at different locations during the stepwise installation. The test bench will consist of all relevant types of diagnostic devices as BPM's, ACCT's, SEM grids, a slit-grid emittance device and a bunch shape monitor. Moreover, a magnetic spectrometer is supposed to measure the energy spread of the proton beam. Point-to-point imaging is foreseen to enable high energy resolution independently on the transverse emittance. Due to the limited space in the accelerator tunnel a special design must be chosen with the inclusion of quadrupole magnets. The present contribution gives an overall presentation of the test bench and its devices with a special emphasis on the magnetic spectrometer design.

INTRODUCTION

The FAIR [1] facility, presently under construction at GSI Darmstadt, is envisaged to provide both antiproton and ion beams. FAIR's accelerator complex will include two linacs as injectors: the existing UNILAC [2] and the pLinac [3], a new proton linac under construction. Both linacs inject into the present SIS18 synchrotron, which will act as an injector for the future SIS100 synchrotron.

The pLinac will consist of an RFQ followed by two 9 m long sections of Cross-bar H-drifttube (CH) accelerating structures working at 325.224 MHz and is designed to deliver a beam current of up to 70 mA at a macropulse length of 36 µs and a typical bunch length of 100 ps [3,4]. The design energy is 68 MeV.

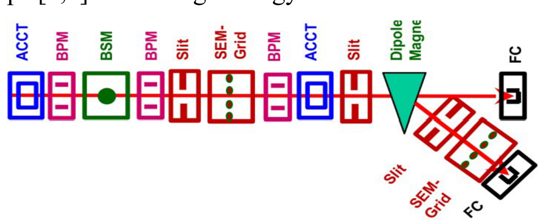

Figure 1: Schematic test bench overview.

During the stepwise commissioning phase a movable test bench will be employed to characterize the proton beam behind each cavity. The bench is foreseen to consist of all relevant types of diagnostic devices that have been developed for the pLinac (BPM's, ACCT's, SEM grids, a slit-grid emittance device and a bunch shape monitor) and additionally a magnetic spectrometer for measurements of the proton beam's energy spread. An overview of the planned bench is shown in Fig. 1.

†s.udrea@gsi.de

STANDARD BEAM DIAGNOSTICS

We give here short descriptions of the main diagnostic devices which will also be installed along the pLinac beam line. For more details see [4].

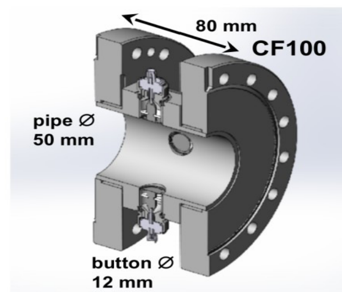

Figure 2: Cross section through a 'beam-line' BPM.

BPMs

The BPMs are of the button type and will be built in two mechanical designs – 'inter-tank' and 'beam-line' – and five different geometries. The 'inter-tank' ones are supposed to be mounted between the CH modules of the CH tanks while the 'beam-line' BPMs will be installed outside the tanks. For the test bench three 'beam-line' BPMs are foreseen with inner diameters of 50 mm and 12 mm wide buttons, see Fig. 2. They will be used both for position and mean energy measurements by the time of flight method [5].

ACCTs

The AC beam transformers (ACCTs) are built by Bergoz (see Fig. 3), were developed based on GSI specifications and are an improvement of a standard Bergoz model. The enhanced ACCT mainly differs from its predecessor by a larger bandwidth (3 MHz instead of 1 MHz), three measurement ranges (100/10/1 mA) instead of one, the availability of a test input and an improved magnetic shielding [6].

Figure 3: The ACCT developed by the Bergoz company.

ISBN: 978-3-95450-204-2 ISSN: 2673-5350 doi:10.18429/JACoW-IBIC2019-MOPP038

SEM grids

Secondary electron emission (SEM) grids are key to beam alignment, quadrupole settings, and, in combination with appropriate slits, emittance measurements. The relatively small transversal size of the proton beam ($\sigma_x \times \sigma_y = 1 \times 1$ mm) and its high current lead to special demands regarding their realisation. While the standard GSI design relies on a well known and proven technology it offers just 1 mm spatial resolution. The technology used at CERN for the LINAC4 [7] or by NTG for ALPI Legnaro offers resolutions down to 0.25 mm but causes some problems at high duty cycles due to thermal expansion and resulting shortcuts between the wires. Also aging effects might play a role after long term operation. Thus there is still development and optimisation work to be done regarding these devices.

BSM

The bunch shape monitor (BSM) is a turn-key 'Feschenko'-type device developed and built by INR/Moscow [8], see Fig. 4. One such unit was successfully commissioned in 2016 at GSI's cw-LINAC prototype. A resolution of approximately 1° has been demonstrated [9].

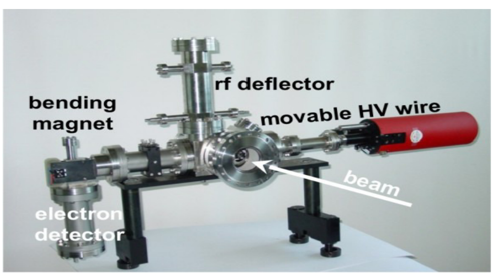

Figure 4: A typical 'Feschenko'-type BSM.

Faraday Cup

To measure the transversal beam distribution at the image plane of the magnetic spectrometer a Faraday cup and a slit will be installed at the appropriate position. The Faraday cup will be realised at GSI Darmstadt based on known technology. It will also act as a beam dump.

THE MAGNETIC SPECTROMETER

To assess the proton beam's energy spread a magnetic spectrometer will be integrated into the test bench. This device is presently in the design phase.

The spectrometer should meet the following requirements:

- capability to work for proton energies from ≈3 MeV up to ≈70 MeV
- compatibility with the further test bench installation
- low space demands especially to the side, since the distance from beam line to the tunnel's wall is only 2.5 m
- resolving power, p/dp, of at least 4000
- if possible, realization with already available components, since the test bench is needed during commissioning.

Since the test bench has to be movable, the spectrometer's design should be kept as simple as possible. To do so one could simply use a pair of slits separated by a certain drift length and followed by a dipole as dispersive element. The slit pair would limit the emittance of the beam reaching the dipole and eventually allow for a good resolving power. As an example we consider here two slits followed by a 90° sector dipole (a dipole's dispersion increases with deflection angle). Let δ be the width of the slits, D the distance between them, L_0 the drift from the second slit to the sector's start, L the distance from the sector's end to the detector and R the sector's bending radius. The distance from the detector to the beam line is $\Delta = R+L$. Assuming the acceptance of the two slits gets filled by the (selected) beam, it can be shown that the maximum first order resolving power is:

$$\frac{p}{dp}=\frac{R\cdot(R+L)}{L\cdot\delta} \quad (1)$$

For L given by:

$$L=\frac{R^2}{D+L_0} \quad (2)$$

One can for instance exceed a resolving power of 4000 by setting D = 2 m, L_0 = 0.5 m, R = 1 m and δ = 0.85 mm. Under these conditions L = 0.4 m and Δ = 1.4 m. Note that the values for D, L_0 and δ have to be such that there are no beam losses within the dipole. A simple and conservative estimate of the lower limit for the dipole's horizontal aperture A_p can be obtained by neglecting the dipole's focussing properties half-way into it:

$$A_p>\delta\cdot\left(1+2\frac{L_0+(\pi/4)\cdot R}{D}\right) \quad (3)$$

An issue of such a two-slit set-up is the need for a very good alignment of both the two narrow slits and the beam. To avoid this, one can use a single slit and the focussing properties of a sector dipole to create a point-to-point image of the slit. This way there is no dependence of the position of an ion at the detector on the angle of its trajectory with the optical axis at the slit. As a consequence, the resolving power has the same expression as in Eq. (1) but L has to satisfy:

$$L\cdot L_0=R^2 \quad (4)$$

Since there is just one slit, one needs to use quadrupoles to prepare the beam in such a way as to have a low enough horizontal divergency. Equation 5 shows the condition that A_p has to satisfy in this case.

$$A_p>\delta+2\,\alpha_{max}\cdot[L_0+(\pi/4)\cdot R] \quad (5)$$

α_{max} is the largest angle (absolute value) within the phase space region selected by the slit.

ISBN: 978-3-95450-204-2 ISSN: 2673-5350 doi:10.18429/JACoW-IBIC2019-MOPP038

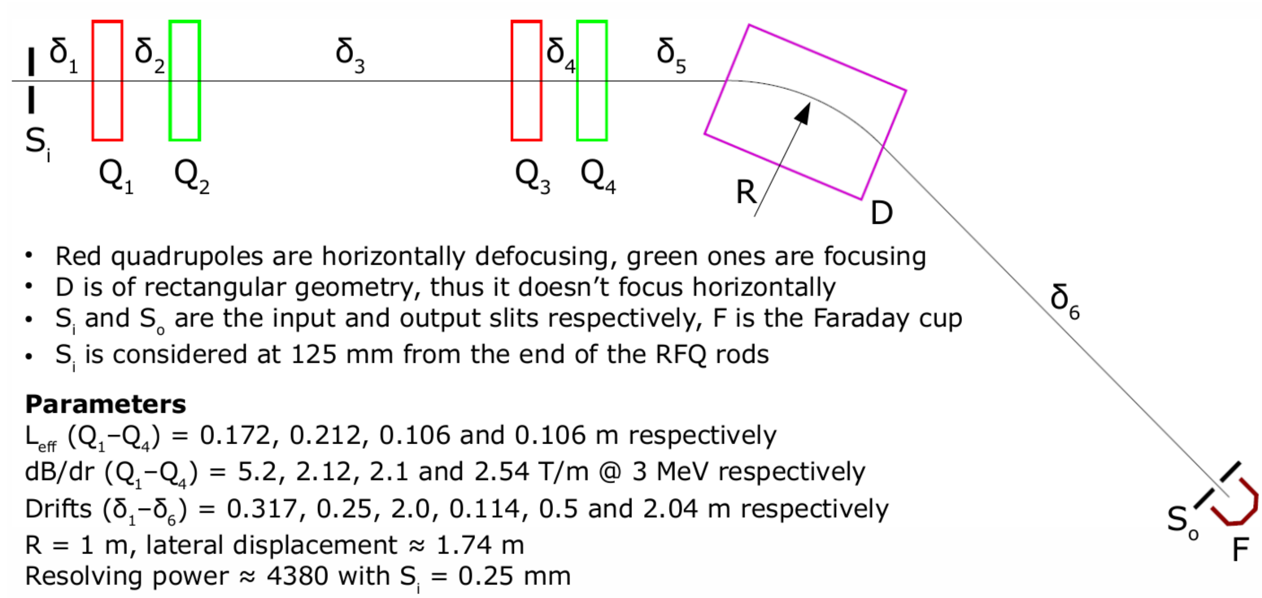

Figure 5: The proposed spectrometer ion optical layout. For the spectrometer to work with 70 MeV protons the field gradients of the quadrupoles would need to be multiplied by a factor of ≈4.8. This leads to values well below the maximums specified by the manufacturer. Moreover the dipole is designed to work up to (at least) this energy.

A set-up involving quadrupoles is more complex than one involving only slits. Nonetheless, especially because of the large divergence of the beam exiting the RFQ and the fact that the test bench has to accommodate also all the other diagnostic devices, quadrupoles are practically unavoidable.

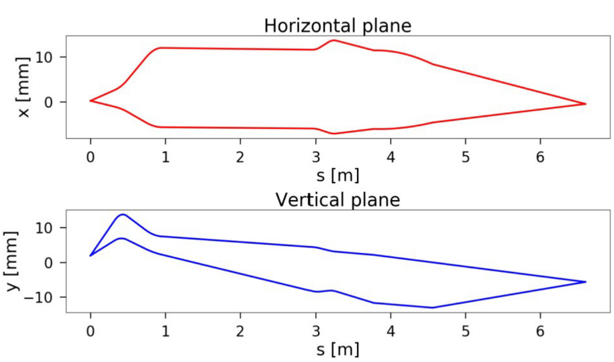

Figure 6: Particle trajectories showing focussing in both planes.

It should be noted here that a set-up using a sector dipole alone as focussing element will not focus in the vertical plane. This might affect the resolving power in case of errors in slit orientation. As a solution, one could employ a double focussing dipole but in this case for a 90° deflection and a typical 1:-1 imaging the lateral deflection Δ would be 3R. Because of the above mentioned space limitations this leads to an upper limit of ≈0.67 m for R and thus the need for a ≈1.8 T field for 68 MeV protons. Since such a strong field is a challenge, quadrupoles could be used to reduce the distance from the dipole's exit to the image plane (i.e. detector), and allow for a dipole with a larger radius, R > 0.81 m.

Several good candidates for the quadrupoles to be installed as part of the spectrometer have been identified at the GSI Darmstadt and MPI for Nuclear Physics in Heidelberg. However neither an appropriate 90° sector nor a double focussing dipole are readily available. Thus a first layout is proposed which uses a 45° rectangular dipole produced and delivered by CEA for guiding the beam from the pLinac into the transfer channel. This layout is presented in Fig. 5. It offers about 2 m of space for installing all other beam diagnostic devices and should achieve a resolving power of about 4380 when using a 0.25 mm slit at the object plane.

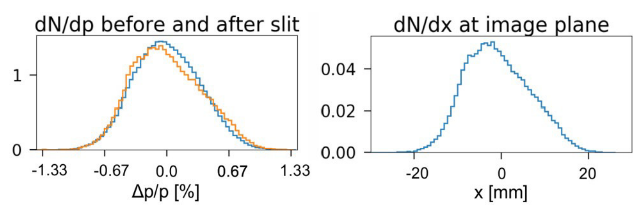

Figure 7: Momentum distribution of the RFQ accelerated beam before (blue) and after (orange) the object plane slit and the beam horizontal distribution at the image plane. The slit is 0.5 mm wide. The distributions are normalized.

The lateral displacement of the beam up to the image plane is approximately 1.74 m, allowing for sufficient free space to the wall. Figure 6 presents simulated particle trajectories, while the horizontal particle distribution at the image plane is shown in Fig. 7. The corresponding computations have been performed with an in-house first order Python [10] based code. Extensive use has been made of the numpy, scipy and matplotlib software packages [11-13]. Input data was taken from the design calculations [14, 15]. More detailed, higher order simulations are planned with the GICOSY [16] and MOCADI [17] codes.

Especially at lower energies the proton beam's energy distribution may change during propagation along the

ISBN: 978-3-95450-204-2 ISSN: 2673-5350 doi:10.18429/JACoW-IBIC2019-MOPP038

beamline due to space charge effects [18]. The effect is visible also in simulations performed at the IAP Frankfurt for the beam exiting the pLinac's RFQ [15]. Figure 8 shows changes expected due to a 125 mm drift from the end of the RFQ rods. Thus the location of the spectrometer's object plane may have a significant influence on the observed energy spectrum.

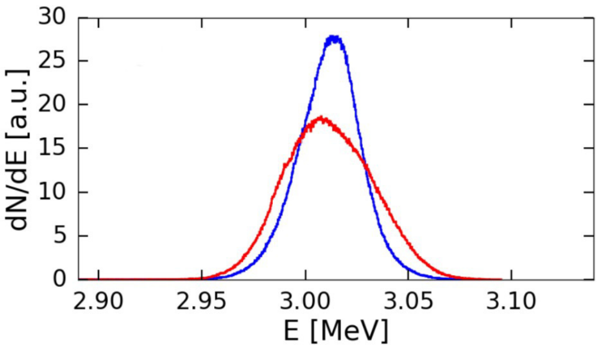

Figure 8: Simulated energy spectrum at the exit of the RFQ (blue) and after a 125 mm drift (red) for a 100 mA beam current [15].

Moreover, due to correlations in the 6D phase space of an RFQ accelerated beam [19], any selection made out of the horizontal phase space is expected to have an influence on the energy distribution measurement. Such an influence has been observed also in the simulated beam, as shown in Fig. 7.

CONCLUSION

For the stepwise commissioning of the future proton injector for FAIR a movable beam diagnostics test bench is under development. While most of its components are also developed and manufactured for the pLinac itself, the foreseen custom magnetic spectrometer will be used during the commissioning phase. First investigations show that it should be possible to achieve the design goals using already available ion optical elements.

ACKNOWLEDGEMENTS

Special thanks go to H. Hähnel for fruitful discussions and for providing the data to be used as input for particle tracking simulations and assess changes in the energy spectrum due to space charge. M. Grieser was instrumental in identifying suitable quadrupoles at the MPI for Nuclear Physics in Heidelberg, while M. Bevcic and C. Mühle helped with the same task at GSI.

REFERENCES

[1] P.J. Spiller *et al.*, "Status of the FAIR Project", in *Proc. IPAC'18*, Vancouver, BC, Canada, Apr. 2018, pp. 63-68. doi:10.18429/JACoW-IPAC2018-MOZGBF2

[2] W. Barth, L. Dahl, L. Groening, S. Yaramishev, and U. Ratzinger, "Long term perspective for the UNILAC as a high current heavy ion injector for the FAIR-accelerator complex", in *Proc. LINAC'06*, Knoxville, Tennessee, USA, Aug. 2006, paper MOP059, pp. 180-182.

[3] C. M. Kleffner *et al.*, "Status of the FAIR pLinac", in *Proc. IPAC'17*, Copenhagen, Denmark, May 2017, pp. 2208-2210. doi:10.18429/JACoW-IPAC2017-TUPVA058

[4] T. Sieber *et al.*, "Beam Diagnostics Layout for the FAIR Proton Linac", in *Proc. LINAC'14*, Geneva, Switzerland, Aug.-Sep. 2014, paper THPP063, pp. 998-1000.

[5] M. H. Almalki *et al.*, "Layout of the BPM system for p-Linac at FAIR and the digital methods for beam position and phase monitoring", in *Proc. IPAC'13*, Oxford, UK, Sep. 2013, paper MOPC21, pp. 101-103.

[6] H. Bayle *et al.*, "Effective shielding to measure beam current from an ion source", *Rev. Sci. Instrum.*, vol. 82, 02A713, 2014. doi:10.1063/1.4829736

[7] B. Cheymol, "Development of beam transverse profile and emittance monitors for the CERN LINAC4", Ph.D. thesis, Université Clermont-Ferrand II - Blaise Pascal, Clermont-Ferrand, France, 2011.

[8] A. V. Feschenko *et al.*, "Technique and instrumentation for bunch shape measurements", in *Proc. RuPAC'12*, Saint Petersbu rg, Ru ssian Federation, Sep. 2012, paper FRXOR01, pp. 181-185.

[9] T. Sieber *et al.*, "Bunch shape measurements at the GSI cw-LINAC prototype", in *Proc. IPAC'18*, Vancouver, BC, Canada, Apr. 2018, pp. 63-68. doi:10.18429/JACoW-IPAC2018-WEPAK006

[10] Python, http://www.python.org/

[11] numpy, https://numpy.org/

[12] scipy, https://www.scipy.org/

[13] matplotlib, https://matplotlib.org/

[14] U. Ratzinger *et al.*, "A 70-MeV proton Linac for the FAIR facility based on CH–cavities", in *Proc. LINAC'06*, Knoxville, Tennessee, USA, Aug. 2006, paper TH1004, pp. 526-530.

[15] H. Hähnel, private communication, Nov. 2018

[16] GICOSY, https://web-docs.gsi.de/~weick/gicosy/

[17] MOCADI, https://web-docs.gsi.de/~weick/mocadi/

[18] G. Bellodi and A. M. Lombardi, "Study of a spectrometer line for the Linac4 diagnostics movable bench", CERN, Geneva, Switzerland, AB-Note-2008-046 ABP, Sep. 2008.

[19] B. Cathey, S. Cousineau, A. Aleksandrov, and A. Zhukov, "First Six Dimensional Phase Space Measurement of an Accelerator Beam", *Phys. Rev. Lett.*, vol. 121, 064804, 2018. doi:10.1103/PhysRevLett.121.064804